IEEE Open Journal of Antennas and Propagation

Received XX Month XXXX; revised X Month XXXX; accepted XX Month XXXX. Date of publication XX Month XXXX; date of current version XX Month XXXX.

Digital Object Identifier 10.1109/OAJPE.2020.2976889

Additively-Manufactured, Magnetically-Controlled, Frequency and Polarization Reconfigurable Phased Array Antenna

ULAN MYRZAKHAN[1], FARHAN A. GHAFFAR[2] (Senior Member, IEEE), MOHAMMAD VASEEM[1], AND ATIF SHAMIM[1] (Fellow, IEEE)

[1]Department of Electrical and Computer Engineering, King Abdullah University of Science and Technology, Thuwal, 23955-6900, Saudi Arabia
[2]Department of Electrical Engineering, Lakehead University, Thunder Bay, ON P7B 5E1, Canada

CORRESPONDING AUTHOR: U. MYRZAKHAN (e-mail: ulan.myrzakhan@kaust.edu.sa).

ABSTRACT An additively manufactured phased array antenna is presented in this work that provides simultaneous reconfiguration in frequency, polarization, and beam direction solely in response to magnetic tuning of the underlying ferrite substrate. This design obviates the need for integrated active components, which have been fundamental elements enabling tuning operation in traditional reconfigurable array antennas. The array element of the proposed array antenna consists of a waveguide-based phase shifter, realized by printing metallic walls on a ferrite substrate, which is then monolithically integrated with a printed circular patch antenna. Depending on the magnitude and polarity of the applied magnetic field (solenoids) to the patches, the array antenna can operate in a linearly polarized (LP) mode at 7.2 GHz or in dual circularly polarized (CP) modes in two continuously tunable frequency bands, 5.9−6.5 GHz and 7.6−7.95 GHz. Simultaneously, when magnetic field is applied to the phase shifters, continuous beam steering within ±25° of the boresight can be realized (±35° when fully saturating the ferrite at the phase shifters). To the best of the authors' knowledge, this is the first implementation of an additively manufactured and fully magnetically controlled array antenna of this versatility.

INDEX TERMS ferrite, frequency reconfigurable, inkjet printing, magnetic material, phased array antenna, polarization reconfigurable, screen printing, YIG.

I. INTRODUCTION

MULTI-reconfigurable antennas have become essential for modern wireless systems that must operate over multiple radios to maximize connectivity [1]. The use of multi-reconfigurable antennas can eliminate the need for multi-antenna systems, offering potential cost and space savings, and enhanced performance across various scenarios [1], [2].

Traditionally, antennas have been made reconfigurable through the use of PIN diodes [3], varactors [4], MEMS devices [5], diversity switches [6], photoconductive switches [7], liquid crystals [8], liquid dielectrics [9], liquid metals [10] or mechanical modifications [11]. Most existing research has focused on single antenna designs with single or dual reconfiguration capability, such as frequency, polarization, or radiation pattern reconfigurability, or a combination of any two of these characteristics. However, single antenna designs often experience lower gain due to a smaller aperture. It has, therefore, become desirable to develop reconfigurable antenna architectures in an array format [12], [13] that, in addition to providing independent tuning in frequency and polarization, can form and steer a narrow beam of higher gain. Despite these significant benefits, very few studies have addressed it. The predominant designs available [14], [15], [16], [17], [18] utilize multiple, independently controlled, on-aperture active components (PIN diodes, varactors etc.) per radiator to achieve independent and simultaneous reconfigurability in frequency, polarization and beam direction, thereby increasing the complexity of the RF and DC circuits. Another proposed design [19] involves reshaping the parasitic array aperture through the use of a stretchable liquid metal. This design, however, suffers from lower switching speeds and requires a considerable number of DC motors for control.

Alternatively, reconfigurable operation in microwaves can be achieved through magnetic tuning of ferrite substrates, eliminating the need for active components and complex RF circuits associated with them. This approach offers the advantages of minituarization [20], and a wide and continuous tuning range, from the unmagnetized to partially magnetized and then to fully saturated states of the ferrite material.

Furthermore, magnetic tuning of ferrites can provide reconfigurability in all three aspects of interest: frequency [21], [22], [23] polarization [24], [25] and phase shifting [26], [27], [28] to realize beam steering array antennas. However, the existing array antenna designs on a ferrite have either targeted switching operations [29], [30] or beam steering alone [31], [32], [33], [34] without the option for frequency and polarization reconfigurability. Moreover, among the existing works, very few [35], [36], [37] have explored the fabrication of ferrite-based antennas using additive manufacturing techniques, despite the importance of additive manufacturing in large-scale and cost-effective production [38], [39]. These gaps highlight an opportunity for further research in this area.

This work aims to address these gaps by utilizing additive manufacturing techniques to realize an array antenna on a ferrite, designed to provide reconfigurability in frequency, polarization and beam direction simultaneously, and solely through magnetic tuning. This work is a comprehensive extension of the work presented in [40]. The array element consists of a waveguide-based phase shifter integrated with a frequency and polarization reconfigurable patch. Depending on the magnitude and polarity of the magnetic field at the patches, the array antenna can operate in a linearly polarized (LP) mode or in dual circularly polarized (CP) modes within two continuously tunable frequency bands. Simultaneously, beam steering can be realized when a magnetic field is applied to the phase shifters. The proposed array antenna achieves the desired multi-reconfigurability while eliminating the need for active components and relies on additive manufacturing, allowing for low-cost and large-scale production.

II. THEORY AND SIMULATIONS

A. MAGNETIC TUNING OF MICROWAVE FERRITES

Ferrite material is characterized as isotropic in the unmagnetized state and anisotropic in the magnetized state. The ferrite in the saturated state can be simulated by assuming Polder's model [41], which is readily available for definition in CST (as a gyrotropic material). This model requires the value of the internal magnetic field, H_0, established inside the ferrite, after the magnetization, M, of the ferrite reaches saturation, M_S.

Ferrites in the partially magnetized state ($0 < M/M_S \leq 1$) can be simulated using Green and Sandy's model [42], which predicts the tensor permeability of the following form for a magnetic bias applied in $\pm z$-direction:

$$[\mu] = \begin{pmatrix} \mu & \pm j\kappa & 0 \\ \mp j\kappa & \mu & 0 \\ 0 & 0 & \mu_Z \end{pmatrix} \tag{1}$$

$$\mu = \mu_0 + (1-\mu_0)\left(\frac{M}{M_S}\right)^{3/2} \tag{2}$$

$$\mu_Z = \mu_0\left(1-\left(\frac{M}{M_S}\right)^{5/2}\right) \tag{3}$$

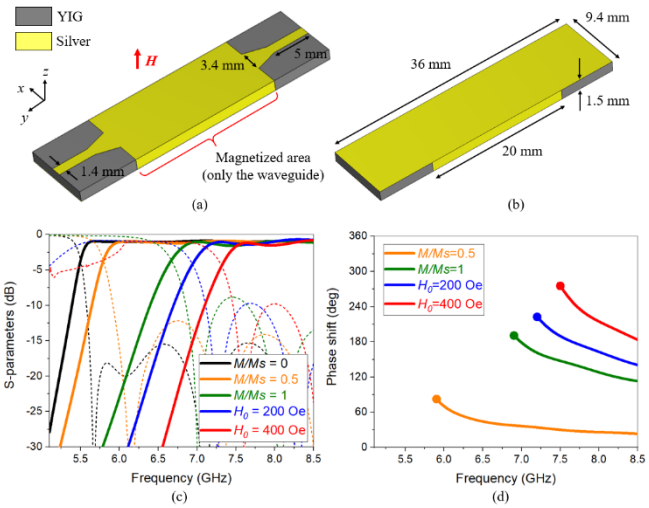

FIGURE 1. (a) Top and (b) bottom views of a waveguide-based ferrite phase shifter. (c) Simulated S_{11} (dashed lines) and S_{21} (solid lines) parameters of the phase shifter for different magnetization states of the YIG inside the waveguide. (d) The simulated phase shifts.

$$\kappa = \frac{\gamma 4\pi M}{f} \tag{4}$$

$$\mu_0 = \frac{1}{3} + \frac{2}{3}\sqrt{1-\left(\frac{f_m}{f}\right)^2} \tag{5}$$

where μ and κ are tensor elements, f is the frequency of operation, and μ_0 is an isotropic permeability of the unmagnetized ferrite, as given by Schlomann's model [42].

These three models are utilized in this work to guide simulations across various magnetization states of the ferrite material, facilitating magnetic tuning.

B. WAVEGUIDE-BASED FERRITE PHASE SHIFTER

To begin with, a rectangular waveguide is designed in CST with metallic walls covering the four sides of a ferrite substrate. This ferrite-loaded waveguide serves as a phase shifter in this work, controlled by a perpendicularly applied DC magnetic field. The DC magnetic field induces and modulates an interaction between the RF wave and the magnetic dipoles of the ferrite, resulting in phase shifting. The waveguide topology is specifically chosen to maximize this interaction, thereby maximizing the phase shifting performance of the device. As for the ferrite material, polycrystalline yttrium iron garnet (YIG) G-113 ($\varepsilon_r = 15$, $\tan\sigma = 2{\cdot}10^{-4}$, $4\pi M_S$ = 1800 G, –3dB ΔH = 24 Oe) from Trans-Tech Inc. is selected. The designed waveguide is then extended by adding waveguide-to-microstrip transitions, as shown in Fig. 1(a) and (b), which are necessary for a planar integration with the antenna. The dimensions of the final structure are optimized assuming unmagnetized conditions ($M/M_S = 0$) of the YIG, and this magnetization state serves as a reference state for the designed phase shifter.

Fig. 1(c) demonstrates the simulated S-parameters of the phase shifter for the unmagnetized, partially magnetized, and fully saturated states of the YIG inside the waveguide. The

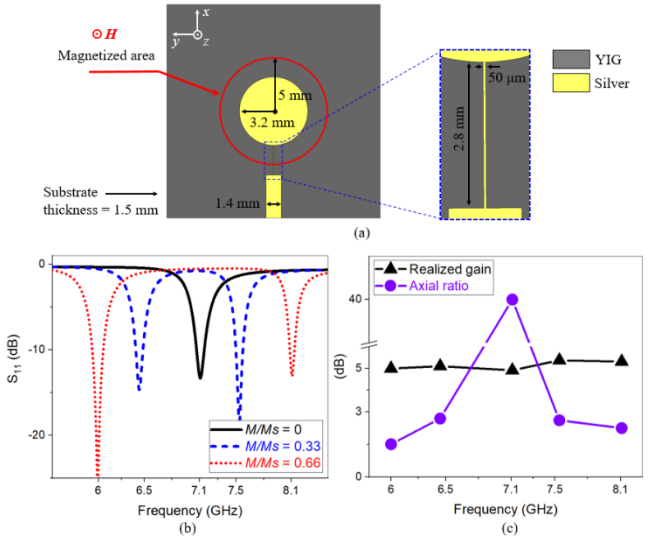

FIGURE 2. (a) Top view of a circular patch antenna on a grounded YIG substrate. (b) Simulated S_{11} parameters of the patch for unmagnetized and +z-directed partially magnetized state of the YIG substrate. (c) Simulated realized gain and AR obtained at every frequency resonance.

fundamental cutoff frequency, f_{TE10}, of the unmagnetized waveguide is designed to appear around 5.6 GHz to ensure operation above magnetization frequency, f_m, (5.04 GHz) of the YIG to avoid its low-field loss. Upon increasing the magnetization ($M > 0$) of the YIG, f_{TE10} shifts to higher frequencies. This behavior is consistent across the partially magnetized and fully saturated states of the YIG and is due to changing effective permeability. As Fig. 1(d) indicates, the stronger the magnetization of the phase shifter, the higher the phase shifts that it can provide. Further details on the operation of the phase shifter can be found in [28].

C. FREQUENCY AND POLARIZATION RECONFIGURABLE PATCH

As the next step, frequency and polarization reconfigurable single antenna must be designed. In this regard, a circular patch antenna is designed on the YIG (Fig. 2(a)). The patch dimensions are optimized for a resonance at 7.1 GHz assuming unmagnetized conditions. The center frequency of 7.1 GHz is chosen for the antenna to allow for frequency tuning (to be discussed in the next paragraph) within the usable band of the phase shifter. A narrow λ/4-transformer is designed to match the 50 Ω feed line with the patch edge. As presented in Fig. 2(b) and (c), under unmagnetized conditions, the antenna element operates in LP mode exhibiting a realized gain of 4.9 dBi.

Upon perpendicularly magnetizing the YIG, the resonant frequency splits into two new resonances, which diverge apart with magnetization, as shown in Fig. 2(b). The realized gain remains around 5 dBi, whereas, the polarization tunes from LP in the unmagnetized state to CP in the magnetized state, with the axial ratio (AR) of less than 3 dB at every tuned resonance (Fig. 2(c)). The frequency splitting occurs due to the induced anisotropy of the YIG, resulting in unequal effective permeability for the two opposite CP waves that make up the original LP wave. In Fig. 2,

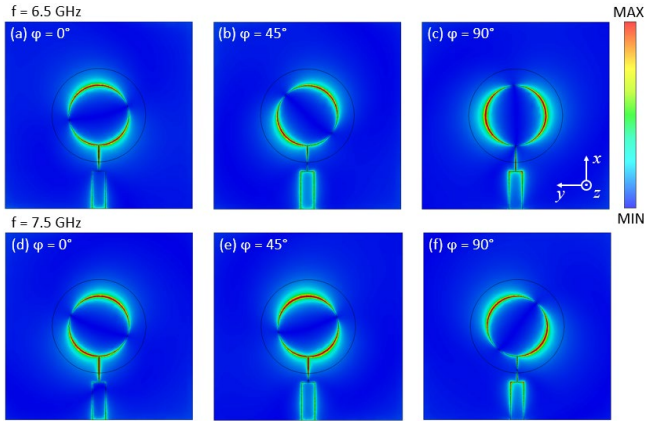

FIGURE 3. Electric field distribution (V/m) at different time instants (viewing the patch from the top) for +z-magnetized YIG (M/M_S = 0.33).

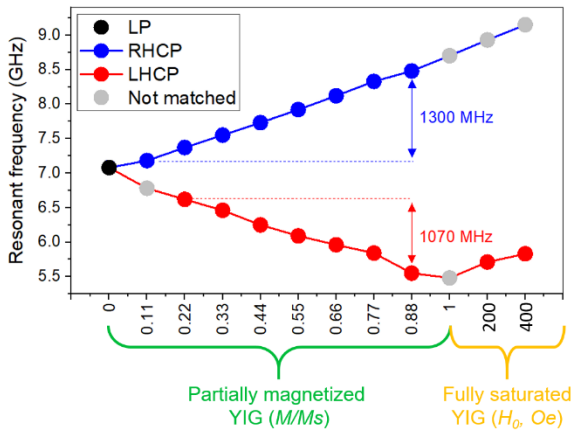

FIGURE 4. Resonant frequency splitting as provided by simulations for a YIG substrate at the patch magnetized in +z-direction.

magnetization in the +z-direction is assumed, leading to left-hand CP (LHCP) at the lower resonance and right-hand CP (RHCP) at the higher resonance. The opposite sense of CP at the two tuned resonances is confirmed by the electric field distribution, depicted at different time instants in Fig. 3 for a magnetization in +z-direction. Changing the direction of magnetization from +z to –z reverses the CP sense at each tuned resonance, but it is not shown here for brevity. This happens because both +z- and –z-directed magnetizations yield the same tensor permeability (1), but with only the sign of the off-diagonal component κ reversed, thereby reversing the anisotropy or the rotational symmetry in *xy*-plane within the YIG.

For a comprehensive analysis, the designed patch antenna is simulated across the full magnetization range of the YIG. As shown in Fig. 4, return loss remains better than 10 dB across the entire partial magnetization range ($0 \le M/M_S \le 1$), except for very low ($M/M_S \le 0.11$) and very high ($M/M_S > 0.88$) values. Simulating the YIG in a fully saturated state tunes the resonant frequency back in the lower band, while further tuning occurs in the higher band, but without impedance match maintained, as demonstrated in the same Fig. 4. These results demonstrate that driving the YIG in the partially magnetized state is sufficient to achieve a wide frequency

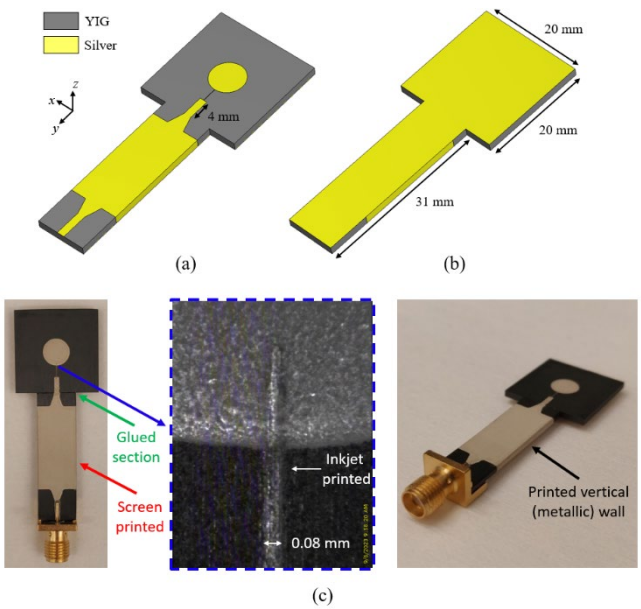

FIGURE 5. (a) Top and (b) bottom geometry of an integrated antenna element. (c) Fabricated prototype.

range (1300 MHz in the higher band and 1070 MHz in the lower band) within which the resonant frequency of the designed patch can be continuously tuned, providing radiation in CP mode (AR ≤ 3 dB), while maintaining the impedance matched.

Following these simulations, the designed phase shifter and the circular patch antenna are integrated, as illustrated in Fig. 5(a) and (b). Three of these integrated antenna elements are used to realize a 1 x 3 phased array antenna. Extensive simulations in CST are conducted to assess the performance of the array in response to different magnetization states of the YIG at the phase shifter and at the patch. The radiation pattern for a single integrated antenna element and the full array are provided in Section IV and will be discussed alongside the measured results.

III. FABRICATION VIA ADDITIVE MANUFACTURING

The proposed array antenna was fabricated through a combination of screen and inkjet printing processes. This combined approach enables the benefits of both the quick printing times of screen printing and the high resolution of inkjet printing. Due to the size limitations of the available YIG substrates (each measuring 36 mm x 20 mm x 1.5 mm), the circular patch and the phase shifter were fabricated separately and then glued together at their intersection, as indicated in Fig. 5(c). However, the need for this manual splicing/glueing can be eliminated by using a YIG substrate of a larger size.

The fabrication begins with screen printing the top and bottom conductors of the integrated antenna element onto the YIG substrate. The resolution of screen printing is limited to 200 µm; therefore, the λ/4-transformer, due to its small width of 50 µm, had to be produced using a more precise inkjet printing technique afterwards. In total, the process involved screen printing 2 layers (approximately 14 µm) of DM-SIP-3072S silver paste from Dycotec Materials [43] and inkjet

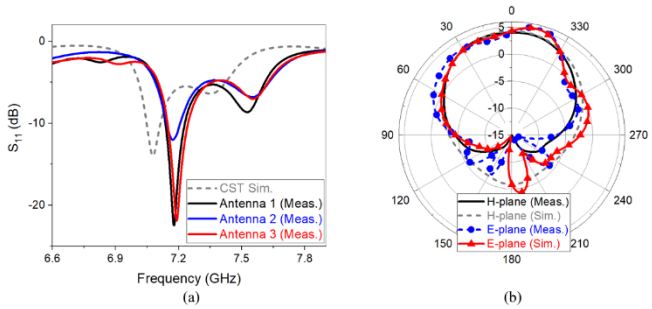

FIGURE 6. Simulated and measured results of integrated antenna elements when no magnetic field is applied: (b) S_{11} parameters and (b) radiation pattern in E- and H-planes.

printing 40 layers (about 6 µm) of SoC ink [44]. Every printed layer had to be dried with IR lamp for about 3 minutes before printing the next layer. The high number of the inkjet-printed layers is primarily due to the narrow width (50 µm) of the λ/4-transformer and the low viscosity of the SoC ink (~5.97x10-3Pa·s [44]). This combination increases the risk of ink spilling beyond the intended area. To prevent this, the waveform of the inkjet printer has been adjusted to reduce the amount of ink jetted with every layer, thus minimizing the chances of spilling, albeit requiring multiple printing layers to realize the desired thickness (~6 µm). To accelerate this process in the future, one can explore the use of high precision dispensing printers [45], which are based on the use of conductive inks (or pastes) of higher viscosity. The final step involved manually printing the vertical sidewalls of the rectangular waveguide with DM-SIP-3072S silver paste. The structure was then placed in a furnace at 150°C for 1 hour to enhance the conductivity of the conducting layers.

The printed prototype with the epoxy-connected SMA connector is depicted in Fig. 5(c). This fabrication process has been repeated to produce the other two copies of the same structure, as required for a 1 x 3 phased array antenna.

IV. MEASUREMENTS

A. SINGLE ANTENNA MEASUREMENTS

The fabricated antenna elements were initially tested individually for their return loss at zero magnetic bias. As shown in Fig. 6(a), a good agreement was achieved among the three antennas, indicating a repeatable and consistent fabrication process. A slight frequency shift between simulations and measurements can be attributed to possible differences between the simulated and actual material properties of the YIG, and the dimensions of the printed layers.

Fig. 6(b) compares the simulated radiation pattern with typical measurements both in E- and H-planes, conducted inside the Satimo Starlab anechoic chamber at zero magnetic bias. The asymmetric shape of the E-plane radiation was investigated through simulations and was primarily attributed to the presence of the phase shifter and the SMA connector in that plane, whose sizes are relatively large compared to the main radiator. To address this asymmetry in the future work, one could design a multilayer structure with the phase shifter in the lower layer and the patch antenna in the upper layer, integrated through a waveguide to coax

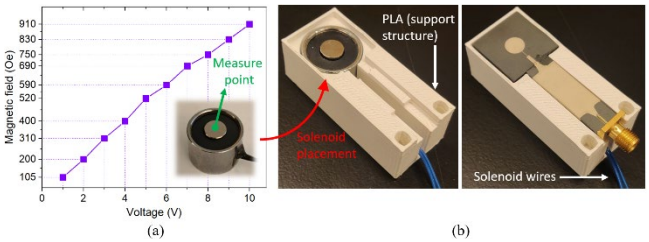

FIGURE 7. (a) Magnetic field generated by solenoid. (b) Placing the integrated antenna element and the solenoid together.

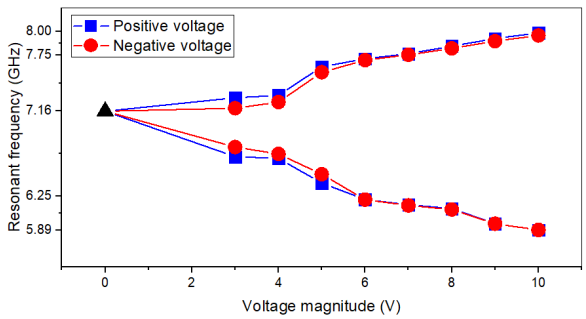

FIGURE 8. Measured resonant frequency splitting as a function of the voltage applied to the solenoid positioned beneath the patch antenna.

transition. This approach shall prevent interference with the radiation of the patch antenna, as an RF ground between the layers would act as an RF shield. For the design considered in this work, a realized gain of 4 dBi and an AR of around 19 dB were measured in the boresight, suggesting a radiation in a LP mode, as expected from the simulations.

To test the antennas under magnetically biased conditions, general-purpose solenoids from Mouser Electronics (#485-3872) were used. The solenoid was measured to generate 910 Oe of magnetic field for maximum applied voltage of 10 V (Fig. 7(a)). This value falls below the magnetic field strength required for saturation, which is approximately 1200 Oe for the YIG of a typical size used in this work [28]. These measurements, therefore, suggest that the selected solenoid will only be able to partially magnetize the YIG substrate, which although limits the tuning, should suffice for a proof of concept.

For ease of handling, a support structure made from polylactic acid (PLA) was 3D printed to securely hold the solenoid and the antenna element together (Fig. 7(b)). As demonstrated in Fig. 8, a split in the operating frequency of the antenna was observed upon activating the solenoid. The *overall* achieved frequency tuning range (5.9 – 8.0 GHz) is less than the range predicted by simulations (5.5 – 8.7 GHz, in Fig. 4) for $0 \leq M/M_S \leq 1$, which, thus, confirms having the YIG only in a partially magnetized state.

Fig. 9 summarizes the measured results of realized gain and AR in the boresight direction. These measurements are only for the applied voltages of positive polarity, which result in $+z$-directed magnetization of the YIG. Analogous results were achieved with negative polarity, but are not shown here to avoid redundancy. As observed in Fig. 9, the AR exhibits a decreasing trend for both the lower and higher resonant frequency regions with the increase in the applied voltage i.e

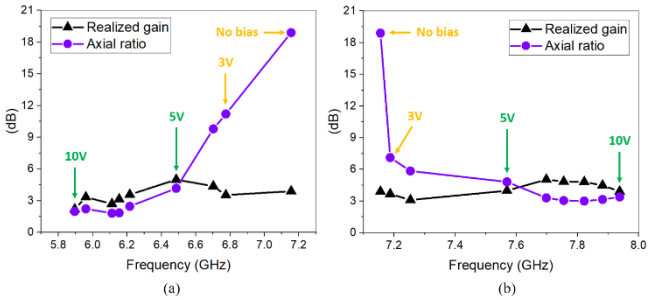

FIGURE 9. Measured realized gain and AR in the boresight direction for (a) lower and (b) higher frequency tuning ranges as a function of positive voltage applied to the solenoid located beneath the patch antenna.

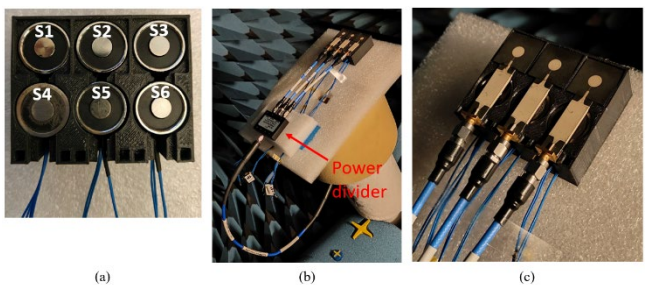

FIGURE 10. (a) Arrangement of the solenoids beneath the proposed phased array antenna. (b), (c) Mounting of the array antenna inside the anechoic chamber, with a feed provided through a three-way power divider.

magnetic field. This trend is expected for AR, as a stronger magnetic field aligns more magnetic dipoles with it, thereby enhancing the purity of the radiating circularly polarized (CP) waves. The optimal performance in terms of measured AR in Fig. 9 was achieved with the bias voltages around 5 V (nominal voltage) and above, which correspond to frequency ranges of approximately 5.9 – 6.5 GHz and 7.6 – 7.95 GHz.

The maximum realized gain of the antenna in Fig. 9 hovers around 3 dBi, deviating to some extent with changes in the applied bias voltage. It is typically higher at the higher resonant frequencies than at the lower. This difference is likely due to the aperture of the patch, which appears electrically smaller at lower frequencies and larger at higher frequencies.

B. ASSEMBLY OF THE ARRAY ANTENNA

After testing the antenna elements individually, they were assembled into a 1 x 3 array to facilitate simultaneous frequency tuning, polarization reconfiguring and beam steering capabilities within a single system (Fig. 10). The spacing between elements was set at 21 mm, which corresponds to a $\lambda/2$ at 7.2 GHz. The array was backed with six identical solenoids: three positioned beneath the patch antennas and three beneath the phase shifters (Fig. 10(a)). The feed was supplied through a three-way SMA power divider (PDM-0618-S3) from RF One [46] (Fig. 10(b)).

C. ARRAY ANTENNA MEASUREMENTS

As shown in Fig. 11(a), in the absence of any magnetic field, the array antenna operates in LP mode, resonating at 7.2 GHz, which matches the resonant frequency of single

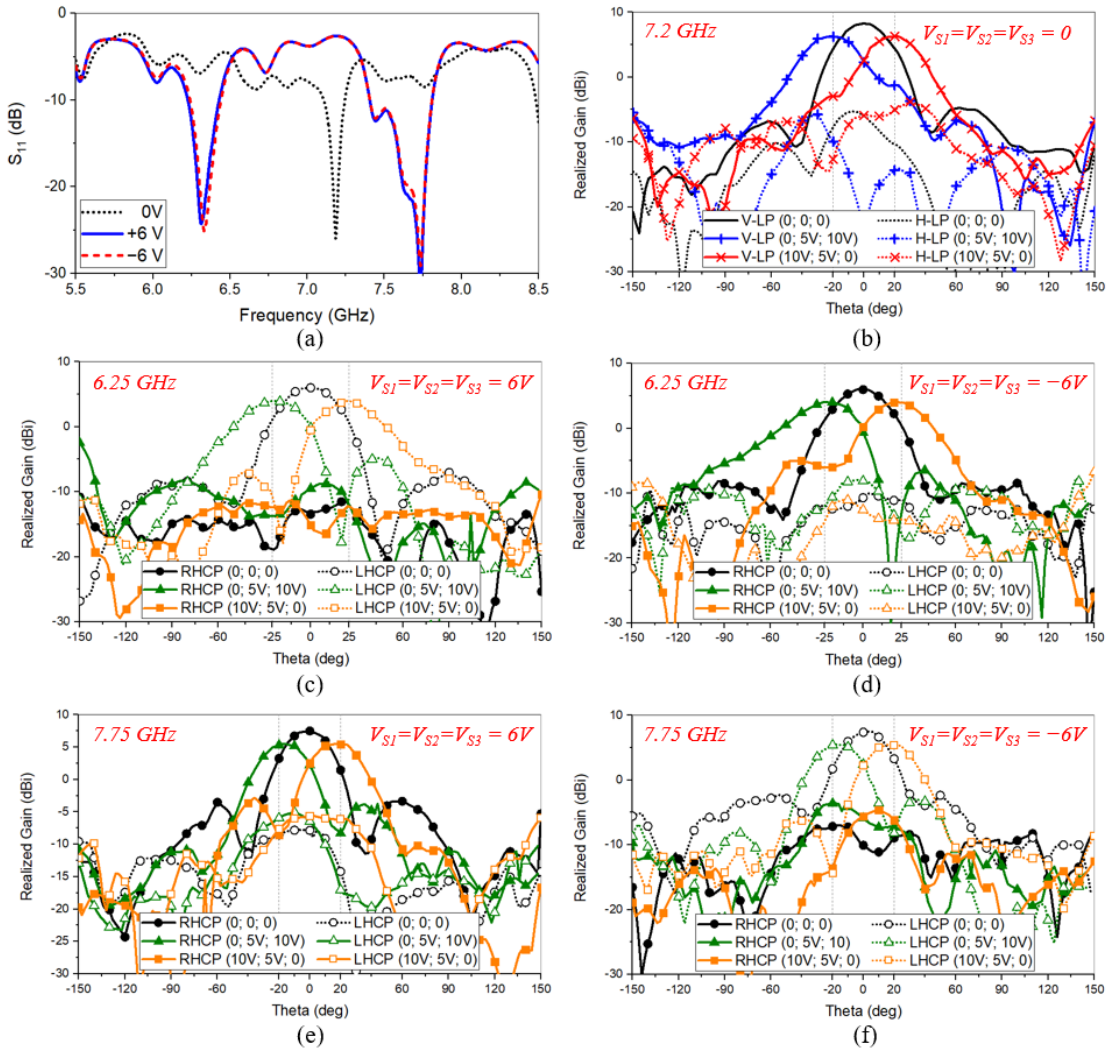

FIGURE 11. Array antenna measurements. (a) S11-parameters for the unbiased and biased states of the YIG at the patches. Beam scanning in (a) LP mode at 7.2 GHz and dual CP mode at (c), (d) 6.25 GHz and (e), (f) 7.75 GHz.

antenna elements (Fig. 6(a)). A scan angle of 20° was achieved in this mode in either directions from the main beam as shown in Fig. 11(b), with a maximum realized gain of 8.3 dBi and maximum side lobe level (SLL) of –13.2 dB. The cross polarization level was measured to reach –14.2 dB with the beam in the boresight. The high cross polarization levels are typical for antennas implemented on ferrite substrates due to gyrotropic nature of this material [22]. During these tests, no power was applied to the solenoids at the patches, while the solenoids at the phase shifters were powered with the voltage sequence of (V_{S4}; V_{S5}; V_{S6}), as indicated in the legend of Fig. 11(b), to produce a progressive phase shift across the array.

The solenoids at the patches were then activated, changing the mode of the array antenna from LP to CP. To streamline the presentation of measurements, this section will focus on a biasing of 6 V across each of the solenoids at the patches. This resulted in a splitting of the resonance frequency to 6.25 and 7.75 GHz (Fig. 11(a)). At the same time, to facilitate beam steering, the solenoids at the phase shifters were powered with the same voltage sequence (V_{S4}; V_{S5}; V_{S6}) as used previously for beam steering in LP mode. Finally, the polarity of the voltage applied to the solenoids at the patches was alternated between –6 V and +6 V to switch between two senses of CP. The measured radiation patterns resulting from these adjustments are displayed in Fig. 11(c), (d) and Fig. 11(e), (f) showcasing beam steering at 6.25 GHz and 7.75 GHz, respectively. The presented results demonstrate a scan angle of ±25° at 6.25 GHz, and ±20° at 7.75 GHz. A comparison of the results in Fig. 11, reveals that the scan angle provided by the proposed phased array antenna reduces as the frequency of operation increases. This outcome is attributed to the inherent characteristics of the designed phase shifter, which exhibits a nonlinear reduction in phase shift with increasing frequency (Fig. 1(d)). This behavior is consistent with the typical traits observed in magnetically tunable phase shifters [27].

A maximum realized gain of 6 and 7.5 dBi was recorded at 6.25 and 7.75 GHz, respectively. The switching of CP is evident in Fig. 11(c) and (d) as well as in Fig. 11(e) and (f),

TABLE 1. Frequency and polarization reconfigurable beam steering array antennas.

Ref. Year	Array Size	Reconfigurability			Tuning elements*	Individual DC bias lines*	Feeding points per radiator	Additively Manufactured
		Freq. Tuning (GHz)	Pol. Tuning	Beam Steering @f_c				
[14] 2016	1 x 4	1.5-2.4	Dual-CP, Dual-LP	±40°	4 varactors, 3 SPDT, 1 diversity RF switch, 1 6-bit phase shifter, 1 6-bit attenuator etc.	>21	2	No
[15] 2018	1 x 2	3.6 5.8	LP, LHCP LP, RHCP	-30°, 0, 30°	5 PIN diodes.	5	1	No
[16] 2021	1 x 4	2.15-2.99	Dual-CP	±40°	8 PIN diodes & 6 varactors.	7	4	No
[17] 2022	4 x 4	1.35-2.19	Triple-LP	±22° (beam splitting)	4 PIN diodes & 4 varactors.	5	4	No
[18] 2014	6 x 6 (parasitic)	2.4-2.9	Dual-CP, Dual-LP	±30°	4 PIN diodes.	4	1	No
[19] 2021	1 x 3 (parasitic)	2.45-6.5	Dual-LP	±45°	~2 LM plugs with 4 DC motors.	4	1	No
[47] 2023	4 x 4	3.43-3.54	Dual-CP	N.A.	4 metal screws#.	N.A (manual control)	1	No
This work	1 x 3	7.2, 5.9-6.5, 7.6-7.95	LP, Dual-CP, Dual-CP	±20° ±25° ±20°	2 solenoids.	4	1	Yes

*per array element; #per complete array.

as the polarity of the voltage across the solenoids S1, S2 and S3 is reversed. The cross polarization of better than –17 dB and –16 dB were achieved for the two hands of CP at 6.25 GHz and 7.75 GHz, respectively, with the beam in the boresight. In this case, SLLs were better than –13 dB and –10 dB at those two frequency resonances, respectively.

It should be noted that while the presented results focus on applying ±6 V to the solenoids at the patches and demonstrating measurements at two specific tuned frequencies, similar reconfigurable performance can be achieved at other frequencies within the tunable spectrum from 5.9 to 6.5 GHz and from 7.6 to 7.95 GHz.

Table I compares the performance of the proposed reconfigurable array antenna with state-of-the-art. As can be seen, traditional array antennas with reconfigurable frequency, polarization and beam direction have predominantly been implemented using active components. The reported designs can be claimed to have achieved independent tuning of three parameters at the cost of integrating multiple active components per radiator, both on the aperture and in the feeding network. Most of the active components have also been provided with individual DC bias lines to independently reconfigure the three parameters of interest. These requirements increase the RF and DC circuit complexity both in the design and fabrication stages. In contrast, the alternative design proposed in this work alleviates the need for active components and complex circuit associated with them, while providing the desired multi-reconfigurable performance through magnetic tuning alone. The proposed design features an RF circuit that is completely isolated from the DC control unit (solenoids), allowing them to be developed and optimized separately, thereby simplifying the design and fabrication processes. It benefits from the anisotropic nature of the YIG, enabling control through both the direction and strength of the applied magnetic field, thereby reducing the number of tuning units and DC bias lines required. The proposed design is also the only one that can be fabricated through additive manufacturing techniques, which highlights its viability for potential low-cost and mass manufacturability.

D. DISCUSSION

Although the desired multi-reconfigurable performance has been achieved, the measured beam scanning capability of the proposed phased array antenna is relatively low. This can be enhanced by driving the YIG substrate at the phase shifters into a fully saturated state. This can be demonstrated through simulations. The simulation model was first validated by comparing the simulated and measured radiation patterns in LP mode, both with the beam directed towards the boresight and at its maximum scan angle. The partial magnetization value (M/Ms) of the YIG at the phase shifter, necessary for the simulations, was determined by correlating the strength of the magnetic field generated by the solenoid in Fig. 7(a) with the $M(H)$ from prior work on the phase shifter [28]. As illustrated in Fig. 12(a) and (b), a satisfactory match was obtained in both scenarios.

The proposed phased array antenna was then evaluated for its maximum scan angle. Simulations revealed that the maximum H_0 value applicable to the phase shifter before its cutoff frequency, f_{TE10}, approaches the frequency of interest (7.2 GHz for LP mode), is around 200 Oe, resulting in a

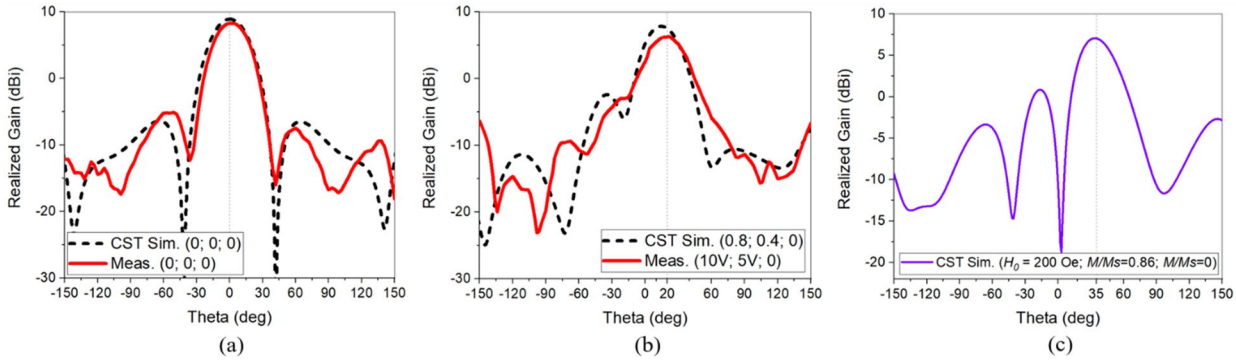

FIGURE 12. Measured and simulated H-plane patterns in LP mode at 7.2 GHz for radiation at (a) boresight and (b) maximum scan angle. (c) Enhanced scan angle achieved in simulations that assume saturated ferrite at the phase shifters.

phase shift of 222° (Fig. 1(d)). The central phase shifter was then modeled in a partially magnetized state (M/Ms = 0.86) to yield half of that phase shift (111°). Biasing the three phase shifters with these values (H_0 = 200 Oe, M/Ms = 0.86, 0) enabled the generation of a maximum phase shift ($\Delta\phi$) between adjacent antenna elements in the array, thereby increasing the scan angle to ±35°, as demonstrated in Fig. 12(c). This is close to the theoretically predicated ($\Delta\phi = \pi sin\theta$) scan angle, θ, of ±38°. It is worth noting that the scan angle can be further increased by simply increasing the length of the waveguide section of the phase shifter. For example, given the phase shift per unit length of 111°/cm (222° / 2 cm), a 360° phase shifter can be realized by increasing the length of the waveguide to 3.25 cm. Simulations suggest that with this length of the phase shifter, the beam steering performance of the proposed phased array antenna can improve to ±45°, which should be adequate for most modern wireless applications.

Two solutions can be explored in the future to achieve full tuning range of the YIG experimentally: (1) designing an optimized solenoid capable of providing stronger magnetic fields or (2) embedding biasing coils within the ferrite material at the device level [25], [27], [33], [34]. The latter solution is preferred as it can reduce the biasing requirements and can potentially achieve a better tuning with a lower applied magnetic field strength.

V. CONCLUSION

A versatile array antenna is presented in this work that relies solely on the magnetic tuning of the underlying ferrite substrate to achieve beam steering with simultaneous reconfigurability in frequency and polarization. Such a performance is highly desirable for modern wireless systems. For a proof of concept, the proposed array antenna design is fabricated through additive manufacturing techniques and measured under different strengths of the magnetic field applied. The non-contact nature of the magnetic control employed in this work enables complete isolation between the RF front end and the control unit (solenoids), which thus can be developed and optimized separately. The diverse reconfiguring ability of the proposed array antenna makes it promising to serve the requirements of many modern applications.

REFERENCES

[1] J. Costantine, Y. Tawk, S. E. Barbin and C. G. Christodoulou, "Reconfigurable Antennas: Design and Applications," in *Proceedings of the IEEE*, vol. 103, no. 3, pp. 424-437, March 2015.

[2] N. Ojaroudi Parchin, H. Jahanbakhsh Basherlou, Y. I. Al-Yasir, A. M. Abdulkhaleq, and R. A. Abd-Alhameed, "Reconfigurable antennas: Switching techniques—A survey," *Electronics*, vol. 9, no. 2, p. 336, 2020.

[3] Symeon Nikolaou *et al.*, "Pattern and frequency reconfigurable annular slot antenna using PIN diodes," in *IEEE Trans. Antennas Propag.*, vol. 54, no. 2, pp. 439-448, Feb. 2006.

[4] J. Zhang, S. Yan and G. A. E. Vandenbosch, "A Low-Profile Frequency Reconfigurable Antenna with Polarization and Pattern Diversity," *2019 IEEE MTT-S International Conference on Microwaves for Intelligent Mobility (ICMIM)*, Detroit, MI, USA, 2019, pp. 1-4.

[5] H. Rajagopalan, J. M. Kovitz and Y. Rahmat-Samii, "MEMS Reconfigurable Optimized E-Shaped Patch Antenna Design for Cognitive Radio," in *IEEE Trans. Antennas Propag.*, vol. 62, no. 3, pp. 1056-1064, March 2014.

[6] H. Luyen, J. H. Booske and N. Behdad, "2-Bit Phase Quantization Using Mixed Polarization-Rotation/Non-Polarization- Rotation Reflection Modes for Beam-Steerable Reflectarrays," in *IEEE Trans. Antennas Propag.*, vol. 68, no. 12, pp. 7937-7946, Dec. 2020.

[7] Y. Tawk, A. R. Albrecht, S. Hemmady, G. Balakrishnan and C. G. Christodoulou, "Optically Pumped Frequency Reconfigurable Antenna Design," in *IEEE Antennas Wireless Propag. Lett.*, vol. 9, pp. 280-283, 2010.

[8] D. Jiang *et al.*, "Liquid Crystal-Based Wideband Reconfigurable Leaky Wave X-Band Antenna," in *IEEE Access*, vol. 7, pp. 127320-127326, 2019.

[9] Z. Chen, H. -Z. Li, H. Wong, X. Zhang and T. Yuan, "A Circularly-Polarized-Reconfigurable Patch Antenna With Liquid Dielectric," in *IEEE Open Journal Antennas Propag.*, vol. 2, pp. 396-401, 2021.

[10] Y. Liu, Q. Wang, Y. Jia and P. Zhu, "A Frequency- and Polarization-Reconfigurable Slot Antenna Using Liquid Metal," in *IEEE Trans. Antennas Propag.*, vol. 68, no. 11, pp. 7630-7635, Nov. 2020.

[11] I. T. McMichael, "A Mechanically Reconfigurable Patch Antenna With Polarization Diversity," in *IEEE Antennas Wireless Propag. Lett.*, vol. 17, no. 7, pp. 1186-1189, July 2018.

[12] M. Ikram, N. Nguyen-Trong and A. Abbosh, "A Simple Single-Layered Continuous Frequency and Polarization-Reconfigurable Patch Antenna Array," in *IEEE Trans. Antennas Propag.*, vol. 68, no. 6, pp. 4991-4996, June 2020.

[13] R. -S. Chen et al., "Reconfigurable Full-Metal Circularly-Polarized Cavity-Backed Slot Antenna and Array With Frequency and Polarization Agility," in *IEEE Trans. Circuits Systems II: Express Briefs*, vol. 70, no. 2, pp. 531-535, Feb. 2023.

[14] B. Babakhani, S. K. Sharma and N. R. Labadie, "A Frequency Agile Microstrip Patch Phased Array Antenna With Polarization

Reconfiguration," in *IEEE Trans. Antennas Propag.*, vol. 64, no. 10, pp. 4316-4327, Oct. 2016.
[15] Y. Panneer Selvam et al., "A Patch-Slot Antenna Array With Compound Reconfiguration," in *IEEE Antennas Wireless Propag. Lett.*, vol. 17, no. 3, pp. 525-528, March 2018.
[16] J. Hu, X. Yang, L. Ge, Z. Guo, Z. -C. Hao and H. Wong, "A Reconfigurable 1 × 4 Circularly Polarized Patch Array Antenna With Frequency, Radiation Pattern, and Polarization Agility," in *IEEE Trans. Antennas Propag.*, vol. 69, no. 8, pp. 5124-5129, Aug. 2021.
[17] J. Wu, X. Lu, W. Wang, J. Han, G. Xu and Z. Huang, "Design of a Compact Polarization-Agile and Frequency-Tailored Array Antenna With Digital-Controllable Radiation Beams," in *IEEE Trans. Antennas Propag.*, vol. 70, no. 2, pp. 813-822, Feb. 2022.
[18] D. Rodrigo, B. A. Cetiner and L. Jofre, "Frequency, Radiation Pattern and Polarization Reconfigurable Antenna Using a Parasitic Pixel Layer," in *IEEE Trans. Antennas Propag.*, vol. 62, no. 6, pp. 3422-3427, June 2014.
[19] V. T. Bharambe, J. Ma, M. D. Dickey and J. J. Adams, "RESHAPE: A Liquid Metal-Based Reshapable Aperture for Compound Frequency, Pattern, and Polarization Reconfiguration," in *IEEE Trans. Antennas Propag.*, vol. 69, no. 5, pp. 2581-2594, May 2021.
[20] S. Jemmeli, T. Monediere, E. Arnaud and L. Huitema, "Ultra-Miniature and Circularly Polarized Ferrite Patch Antenna," in *IEEE Trans. Antennas Propag.*, vol. 71, no. 8, pp. 6435-6443, Aug. 2023.
[21] L. -R. Tan, R. -X. Wu, C. -Y. Wang and Y. Poo, "Ferrite-Loaded SIW Bowtie Slot Antenna With Broadband Frequency Tunability," in *IEEE Antennas Wireless Propag. Lett.*, vol. 13, pp. 325-328, 2014.
[22] A. Shamim, J. R. Bray, N. Hojjat and L. Roy, "Ferrite LTCC-Based Antennas for Tunable SoP Applications," in *IEEE Trans. Comp., Packag. Manufact. Techn.*, vol. 1, no. 7, pp. 999-1006, July 2011.
[23] F. A. Ghaffar and A. Shamim, "A self-biased 3D tunable helical antenna in ferrite LTCC substrate," *2015 IEEE Int. Symp. Antennas Propag. & USNC/URSI Nat. Radio Sci. Meeting*, 2015, pp. 2291-2292.
[24] D. M. Pozar, "Radiation and scattering characteristics of microstrip antennas on normally biased ferrite substrates," in *IEEE Trans. Antennas Propag.*, vol. 40, no. 9, pp. 1084-1092, Sept. 1992.
[25] F. A. Ghaffar, J. R. Bray and A. Shamim, "Theory and Design of a Tunable Antenna on a Partially Magnetized Ferrite LTCC Substrate," in *IEEE Trans. Antennas Propag.*, vol. 62, no. 3, pp. 1238-1245, March 2014.
[26] X. Yang et al., "Compact and Low Loss Phase Shifter With Low Bias Field Using Partially Magnetized Ferrite," in *IEEE Trans. Magn.*, vol. 49, no. 7, pp. 3882-3885, July 2013.
[27] A. Nafe and A. Shamim, "An Integrable SIW Phase Shifter in a Partially Magnetized Ferrite LTCC Package," in *IEEE Trans. Microw. Theory Techn.*, vol. 63, no. 7, pp. 2264-2274, July 2015.
[28] U. Myrzakhan, F. A. Ghaffar, M. Vaseem, H. Fariborzi and A. Shamim, "Inkjet-Printed Ferrite Substrate-Based Vialess Waveguide Phase Shifter," in *IEEE Trans. Magn.*, vol. 59, no. 4, pp. 1-12, April 2023.
[29] L. Dixit and P. Pourush, "Radiation characteristics of switchable ferrite microstrip array antenna," *IEEE Proceedings-Microw., Antennas Propag.*, vol. 147, no. 2, pp. 151–155, 2000.
[30] R. Pourush, G. S. Tyagi, G. P. Srivastava and P. K. S. Pourush, "Radiation Performance of Switchable Ferrite Microstrip Array Antenna," in *IEEE Antennas Wireless Propag. Lett.*, vol. 5, pp. 195-198, 2006.
[31] Hoton How, Ta-Ming Fang, Wei Liu, C. Vittoria, M. H. Champion and H. L. Southall, "Antenna array of circular patches on ferrite substrate," in *IEEE Trans. Magn.*, vol. 33, no. 1, pp. 735-738, Jan. 1997.
[32] H. How *et al*., "Steerable phased array antennas using single-crystal YIG phase shifters-theory and experiments," in *IEEE Trans. Microw. Theory Techn.*, vol. 48, no. 9, pp. 1544-1549, Sept. 2000.
[33] A. Nafe, F. A. Ghaffar, M. F. Farooqui and A. Shamim, "A Ferrite LTCC-Based Monolithic SIW Phased Antenna Array," in *IEEE Trans. Antennas Propag.*, vol. 65, no. 1, pp. 196-205, Jan. 2017.
[34] F. A. Ghaffar and A. Shamim, "A Partially Magnetized Ferrite LTCC-Based SIW Phase Shifter for Phased Array Applications," in *IEEE Trans. Magn.*, vol. 51, no. 6, pp. 1-8, June 2015.
[35] A. Nafe, M. Farooqui and A. Shamim, "Tunable inkjet-printed slotted waveguide antenna on a ferrite substrate," 2015 *9th European Conf. on Antennas Propag. (EuCAP)*, 2015, pp. 1-3.
[36] F. A. Ghaffar, M. Vaseem, L. Roy and A. Shamim, "Theoretical Study of Fully Printed Magnetically Tunable Reconfigurable Patch Antenna," 2018 *IEEE Indian Conf. Antennas Propog. (InCAP)*, 2018, pp. 1-4.
[37] E. Andreou, T. Zervos, A. A. Alexandridis, and G. Fikioris, "Analysis, design and fabrication of reconfigurable patch antenna on magnetodielectric composite substrate with biased ferrite particles," *AEU – Int. Journal Electron. Comm.*, vol. 144, p. 154043, 2022.
[38] D. Helena, A. Ramos, T. Varum and J. N. Matos, "Antenna Design Using Modern Additive Manufacturing Technology: A Review," in *IEEE Access*, vol. 8, pp. 177064-177083, 2020.
[39] M. Chakraborty, J. Kettle and R. Dahiya, "Electronic Waste Reduction Through Devices and Printed Circuit Boards Designed for Circularity," in *IEEE Journal Flexible Electronics*, vol. 1, no. 1, pp. 4-23, Jan. 2022.
[40] U. Myrzakhan, F. A. Ghaffar, M. Vaseem, and A. Shamim, "Additively-Manufactured, Magnetically-Controlled Reconfigurable Array Antenna," *2024 54rd European Microwave Conference (EuMC)*, Paris, France, 2024.
[41] D. M. Pozar, "Basic properties of ferromagnetic materials", in *Microwave engineering*. 3rd ed., New York: John Wiley & Sons, 2005, pp. 441–460.
[42] J. J. Green and F. Sandy, "Microwave Characterization of Partially Magnetized Ferrites," in *IEEE Trans. Microw. Theory and Techn.*, vol. 22, no. 6, pp. 641-645, Jun. 1974.
[43] "Ultra high performance conductive silver paste DM-sip-3072s," Dycotec Materials, https://www.dycotecmaterials.com/product/silver-conductive-paste-dm-sip-3072s/ (accessed Jan. 1, 2024).
[44] M. Vaseem, G. McKerricher, and A. Shamim, "Robust design of a particle-free silver-organo-complex ink with high conductivity and inkjet stability for flexible electronics," *ACS Applied Materials & Interfaces*, vol. 8, no. 1, pp. 177–186, 2015.
[45] "Ultra-Precise Dispensing is the cutting-edge nanotechnology achievement, allowing for unparalleled material placement accuracy down to micrometer scales," XTPL, https://xtpl.com/ultra-precise-dispensing/ (accessed Oct. 2, 2024).
[46] "3 way SMA power divider 6-18 ghz," RF ONE Electronics, https://www.rfone.cn/products/3-way-sma-power-divider-6-18-ghz-pdm-0618-s3 (accessed Jan. 1, 2024).
[47] R. -S. Chen et al., "Reconfigurable Full-Metal Circularly-Polarized Cavity-Backed Slot Antenna and Array With Frequency and Polarization Agility," in *IEEE Trans. Circ. Syst*. II: Express Briefs, vol. 70, no. 2, pp. 531-535, Feb. 2023

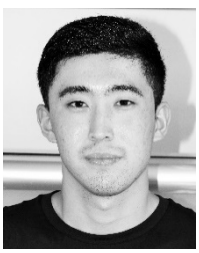

Ulan Myrzakhan received the B.S. degree (with the highest honors) in electrical and electronics engineering from the Nazarbayev University, Astana, Kazakhstan, in 2017, and the M.S. degree in electrical and computer engineering from the King Abdullah University of Science and Technology (KAUST), Thuwal, Saudi Arabia, in 2019. He is currently pursuing the PhD degree within the electrical and computer engineering program at KAUST.

He was an intern in the Academy of Information and Communication Technologies, Taldykorgan, Kazakhstan in 2014. His research interests encompass the design of tunable and reconfigurable microwave devices and antennas, along with their integration into systems, with a focus on utilizing low-cost additive manufacturing techniques for fabrication and ferrite materials for magnetic tuning.

Farhan A. Ghaffar (Senior Member, IEEE) received the B.E. degree in electronics engineering from the NED University of Engineering and Technology, Karachi, Pakistan, in 2007, and the M.S. and Ph.D. degrees in electrical engineering from the King Abdullah University of Science and Technology (KAUST), Thuwal, Saudi Arabia, in 2010 and 2016, respectively.

Before joining Lakehead University as an Assistant Professor with the department of Electrical Engineering, he was working as a Postdoctoral Fellow/Instructor with Ontario Tech University, Oshawa, ON, Canada from January 2017 to July 2019. He was an Assistant Manager with Space and Upper Atmosphere Research Commission (SUPARCO) of Pakistan from 2008 to 2009. He was invited as a Visiting Researcher with Carleton University and Royal Military College, in 2010 and 2012, respectively. He has authored or coauthored more than 40 international publications which includes 20 peer-reviewed journal papers. He is a Co-Inventor on five international patents.

Dr. Ghaffar was the recipient of the Academic Excellence Award at KAUST in 2013 and 2015, secured Honorary Mention in the First Ever 3MT Competition at International Microwave Symposium (IMS) and was awarded best performance award at SUPARCO in 2009. His current research interests include the design of system-on-package and system-on-a-chip-based antennas, radio frequency integrated circuits, flexible microwave passive components, and ferrite low temperature co-fired ceramic-based tunable antennas and passives.

Mohammad Vaseem received the M.Sc. degree in physical chemistry from Aligarh Muslim University (AMU), Aligarh, India, in 2005, and the Ph.D. degree in chemical engineering from Chonbuk National University, Jeonju, South Korea, in 2011.

From 2011 to 2014, he was a Post-Doctoral Fellow in World Class University (WCU) Project and Brain Korea 21 Project with Chonbuk National University. From 2015 to 2018, he was a Post-Doctoral Fellow in the Electrical Engineering Program with the King Abdullah University of Science and Technology (KAUST), Thuwal, Saudi Arabia, where he is currently a Research Scientist. He has authored or coauthored more than 67 international publications, 3 book chapters, and 80 research paper presentation in several national and inter-national conferences. He is an inventor of 5 patents. His current research interests include ink-development for metal, dielectric, oxide semiconductor, magnetic, phase-change material and several other functional materials and its inkjet and screen printing for the fabrication of RF electronics, RF switches, transistors, sensors, and so on.

Atif Shamim received his MS and PhD degrees in electrical engineering from Carleton University, Canada in 2004 and 2009 respectively.

He was an NSERC Alexander Graham Bell Graduate scholar at Carleton University from 2007 till 2009 and an NSERC postdoctoral Fellow in 2009-2010 at Royal Military College Canada and KAUST. In August 2010, he joined the Electrical and Computer Engineering Program at KAUST, where he is currently a Professor and principal investigator of IMPACT Lab. He was an invited researcher at the VTT Micro-Modules Research Center (Oulu, Finland) in 2006. He is an author/co-author of over 300 international publications, an inventor on more than 40 patents and has given 100 invited talks at various international forums. His research interests are in innovative antenna designs and their integration strategies with circuits and sensors for flexible and wearable wireless sensing systems through a combination of CMOS and additive manufacturing technologies.

Dr. Shamim's research work has won best paper awards in IEEE ICMAC 2021, IEEE IMS 2016, IEEE MECAP 2016, IEEE EuWiT 2008, first prize in IEEE IMS 2019 3MT competition and IEEE AP-S Design Competition 2022, finalist/honorable mention prizes in IEEE APS Student paper competition 2022, IEEE AP-S Design Competition 2020, IEEE IMS 2017 (3MT competition), R. W. P. King prize for IEEE TAP 2017 and 2020, IEEE IMS 2014, IEEE APS 2005. He has been selected as the Distinguished Lecturer for IEEE AP-S (2022-2024). He has won the King's Prize for the best innovation of the year (2018) for his work on sensors for the oil industry. He was given the Ottawa Centre of Research Innovation (OCRI) Researcher of the Year Award in 2008 in Canada. His work on Wireless Dosimeter won the ITAC SMC Award at Canadian Microelectronics Corporation TEXPO in 2007. He also won numerous business-related awards, including 1st prize in Canada's national business plan competition and was awarded OCRI Entrepreneur of the year award in 2010. He is a Fellow of IEEE, founded the first IEEE AP/MTT chapter in Saudi Arabia (2013) and served on the editorial board of IEEE Transactions on Antennas and Propagation (2013-2019), and as a Guest Editor for IEEE AWPL Special issue (2019), and is currently serving as an Associate Editor for IEEE Journal of Electromagnetics, RF and Microwaves in Medicine and Biology. He serves on numerous IEEE committees such IEEE Technical committees on Antenna Measurements (AP-S), Microwave Controls (MTT-S 13), and Additive Manufacturing (CRFID).